Microbiology (2010), **156**, 2180–2193 **DOI** 10.1099/mic.0.038331-0

Role of *vimA* in cell surface biogenesis in *Porphyromonas gingivalis*

Devon O. Osbourne,[1] Wilson Aruni,[1] Francis Roy,[1] Christopher Perry,[2] Lawrence Sandberg,[2] Arun Muthiah[1] and Hansel M. Fletcher[1]

Correspondence
Hansel M. Fletcher
hfletcher@llu.edu

[1]Division of Microbiology and Molecular Genetics, School of Medicine, Loma Linda University, Loma Linda, CA 92350, USA

[2]Division of Biochemistry, School of Medicine, Loma Linda University, Loma Linda, CA 92350, USA

Received 19 January 2010
Revised 1 April 2010
Accepted 6 April 2010

The *Porphyromonas gingivalis vimA* gene has been previously shown to play a significant role in the biogenesis of gingipains. Further, in *P. gingivalis* FLL92, a *vimA*-defective mutant, there was increased auto-aggregation, suggesting alteration in membrane surface proteins. In order to determine the role of the VimA protein in cell surface biogenesis, the surface morphology of *P. gingivalis* FLL92 was further characterized. Transmission electron microscopy demonstrated abundant fimbrial appendages and a less well defined and irregular capsule in FLL92 compared with the wild-type. In addition, atomic force microscopy showed that the wild-type had a smoother surface compared with FLL92. Western blot analysis using anti-FimA antibodies showed a 41 kDa immunoreactive protein band in *P. gingivalis* FLL92 which was missing in the wild-type *P. gingivalis* W83 strain. There was increased sensitivity to globomycin and vancomycin in FLL92 compared with the wild-type. Outer membrane fractions from FLL92 had a modified lectin-binding profile. Furthermore, in contrast with the wild-type strain, nine proteins were missing from the outer membrane fraction of FLL92, while 20 proteins present in that fraction from FLL92 were missing in the wild-type strain. Taken together, these results suggest that the VimA protein affects capsular synthesis and fimbrial phenotypic expression, and plays a role in the glycosylation and anchorage of several surface proteins.

INTRODUCTION

A variety of bacterial cell surface components, including capsule, polysaccharides, proteases (gingipains), haemagglutinin, lipopolysacharides (LPSs), major outer-membrane proteins and fimbriae contribute to the virulence of *Porphyromonas gingivalis* (reviewed by Lamont & Jenkinson, 1998; Yoshimura *et al.*, 2009). This organism, a black-pigmented, Gram-negative anaerobe, is an important aetiological agent of periodontal disease and is associated with other systemic illnesses including cardiovascular disease (Dave & Van, 2008; Demmer & Desvarieux, 2006; Ford *et al.*, 2007; Nakano *et al.*, 2009). Cell surface components like the fimbriae (Amano *et al.*, 1999; Murakami *et al.*, 2004; Wang *et al.*, 2009), lectin-like adhesins (Cutler *et al.*, 1995) and gingipains (McAlister *et al.*, 2009; Pavloff *et al.*, 1997; Pike *et al.*, 1996) are integrally involved in the adhesion, invasion and colonization of periodontal tissue. In addition, the gingipains are involved in several cellular processes (Kuramitsu, 1998) including growth, inactivation of cytokines and their receptors, platelet aggregation, attenuation of neutrophil antibacterial activities, increasing vascular permeability, and apoptosis of gingival epithelial cells (Stathopoulou *et al.*, 2009). Gingipains consist of a lysine-specific protease (Kgp) and an arginine-specific protease (Rgp), which is further subdivided into RgpA and RgpB; these proteases cleave proteins after arginine residues, and are encoded by the *rgpA* and *rgpB* genes, respectively. The mature form of RgpA contains a catalytic domain and a haemagglutinin domain, while RgpB possesses only a catalytic domain. Lysine-specific protease (Kgp) (Imamura, 2003; Mikolajczyk-Pawlinska *et al.*, 1998; Pavloff *et al.*, 1995) cleaves proteins after lysine residues.

Post-translational modifications of surface components such as gingipains, fimbriae and LPS play a key functional role in regulating the virulence of the organism. The maturation pathways of the gingipains are linked to the biosynthesis of surface carbohydrates (Paramonov *et al.*, 2005; Shoji *et al.*, 2002) and several other proteins, including PorR (Shoji *et al.*, 2002), PorT (Nguyen *et al.*, 2009; Sato

Abbreviations: ABA, *Agaricus bisporus* lectin; AFM, atomic force microscopy; BHI, brain–heart infusion; ConA, Concanavalin A; DBA, *Dolichos biflorus* lectin; ECA, *Erythrina cristagalli* lectin; LPA, *Limulus polyphemus* lectin; LPS, lipopolysaccharide; MS, mass spectrometry; PAD, peptidyl arginine deiminase; SBA, *Glycine max* lectin; TEM, transmission electron microscopy; TLCK, *N*-α-*p*-tosyl-L-lysine chloromethyl ketone; TSBKH, trypticase soy broth containing menadione and haemin; WTA, *Triticum vulgaris* lectin.

et al., 2005), Sov (Sato *et al.*, 2005) and VimA (Vanterpool *et al.*, 2004, 2005b, 2006). Arg-X also plays a role in processing fimbriae protein precursors, serving as a proteinase for fimbrillin maturation (Kato *et al.*, 2007; Nakayama *et al.*, 1996). The LPS of *P. gingivalis*, which has recently been shown to contain two macromolecules [O-LPS (O antigen attached to a lipid A core) and A-LPS (phosphorylated branched mannan repeating unit attached to a lipid A core)], undergoes several stages of assembly, including catalysis by a relaxed-specificity ligase which is able to attach either a branched phosphorylated mannan or a tetrasaccharide repeating unit to the Lipid A core (Rangarajan *et al.*, 2008). Lipid A is also present in several structural forms (Kumada *et al.*, 1995) and probably functions in response to strain differences as well as environmental cues.

The *P. gingivalis vimA* gene, which is part of the *recA* operon and codes for a 39 kDa protein (putative acyl-CoA *N*-acyltransferase) has been previously shown to be part of the maturation pathway for gingipains (Abaibou *et al.*, 2001; Vanterpool *et al.*, 2006). Though the mechanism for gingipain regulation has not been thoroughly elucidated, we have demonstrated that *vimA* modulates the phenotypic expression of the gingipains. Additionally, inactivation of this gene resulted in a non-black pigmented strain designated *P. gingivalis* FLL92, which showed reduced levels of proteolytic, haemagglutinating and haemolytic activities (Abaibou *et al.*, 2001; Olango *et al.*, 2003). Using a mouse model, the virulence of *P. gingivalis* FLL92 was shown to be drastically reduced when compared with wild-type W83 strain. The reduced proteolytic activity observed in this *vimA*-defective mutant is as a result of a defect in the post-translational regulation of the gingipain genes. This is further supported by the presence of the pro-enzyme form of the gingipains in addition to their unaltered transcription in the *vimA*-defective mutant (Olango *et al.*, 2003). There is also a late onset of gingipain activity in FLL92, which is mostly soluble, with little or no cell-associated activity (Olango *et al.*, 2003; Vanterpool *et al.*, 2005b). Other studies have shown that the recombinant VimA can interact with the gingipains in addition to several proteins, including HtrA, β-lactamase and sialidase, which are known in other bacterial systems to be involved in post-translational regulation (Vanterpool *et al.*, 2006). It still remains unclear whether the *vimA* gene product is part of a central mechanism that may be involved in the maturation or post-translational regulation of other cell surface proteins in *P. gingivalis*.

In the present study, we further characterized the cell surface of the *vimA*-defective mutant of *P. gingivalis*. We investigated the role of VimA on capsule and fimbriae formation and outer-membrane protein expression. In addition, the effect of cell surface changes on antibiotic resistance was also evaluated.

METHODS

Bacterial strains and growth conditions. *P. gingivalis* strains (W83, ATCC 33277 and FLL92) were grown in either brain–heart infusion (BHI) broth (Difco) supplemented with cysteine (0.1 %), vitamin K (0.5 μg ml^{-1}) and haemin (5 μg ml^{-1}) (BHI-HK) or trypticase soy broth containing menadione and haemin (TSBKH). Solid medium was prepared by supplementing with 1.5 % agar and 5 % defibrinated sheep blood (Haemostat laboratories). All cultures were incubated at 37 °C in an anaerobic chamber (Coy Manufacturing) in 80 % N_2, 10 % H_2 and 10 % CO_2. Growth rates were determined spectrophotometrically at 600 nm (OD).

Biofilm formation assay. Biofilm formation was assayed in 96-well microtitre dishes (R. J. Lamont, personal communication). Briefly, *P. gingivalis* was cultured overnight in TSBKH media. One millilitre of the overnight culture (mid-exponential phase) was centrifuged at 12 851 r.c.f. for 2 min at room temperature. The pellet was collected and washed twice with 1 ml PBS, then resuspended in a 1 ml mixture of TSBKH and PBS (1 : 2). Aliquots of the sample were added to each well. Plates were then incubated with a slight rotation for 24 h in an anaerobic chamber, to allow for the development of biofilm. After removal of the culture supernatant, the plates were washed twice by immersion in distilled water, then allowed to air dry for 1 h. The biofilm was stained with 0.5 % safranin for 15 min (100 μl per well), then washed twice with distilled water. Ethanol (95 %) was added to solubilize the safranin which was transferred to a new microtitre dish. Biofilm formation was obtained by determining the absorbance with a plate reader at 490 nm (Davey & Duncan, 2006).

Analysis of *P. gingivalis* strains by RT-PCR. Total RNA was extracted from *P. gingivalis* at the early (OD_{600} 1.0) phase of the growth cycle, using the SV total RNA isolation system (Promega). RT-PCR was performed using primers specific for the FimA (forward, 5′-GGCAGAACCCGTTGTAGAAA; reverse, 5′-GACCAAAGAATT-GCCGAAAA) and 16S ribosomal (Bogen & Slots, 1999) gene product and the one-step RT-PCR kit (Invitrogen), following the manufacturer's instructions, with 1 μg template RNA in 50 μl RT-PCR mixture. RT-PCR in the absence of reverse transcriptase served as the negative control.

Protein electrophoresis and blotting. SDS-PAGE was performed according to the manufacturer's instructions (Invitrogen) on 10 % Bis/Tris separating gel in morpholinepropanesulfonic acid (MOPS) SDS running buffer. Proteins separated by SDS-PAGE were electrophoretically transferred to a nitrocellulose membrane (Whatman Optitran BA-S 85) and the blotted membranes were immunostained with polyclonal anti-FimA antibody (Lin *et al.*, 2006). Studies using lectin from *Agaricus bisporus* [ABA; specific for galactose (β 1,3) *N*-acetylgalactosamine], Concanavalin A (ConA; specific for α-mannose and α-glucose), *Dolichos biflorus* (DBA; specific for *N*-acetyl-α-D-galactosamine), *Erythrina crista-galli* [ECA; specific for galactose (β 1,4) *N*-acetylglucosamine], *Glycine max* [SBA; specific for *N*-acetyl-D-galactosamine], *Limulus polyphemus* [LPA; specific for sialic acid (*N*-acetyl neuraminic acid)] and *Triticum vulgaris* [WGA; specific for *N*-acetyl-β-D-glucosamine] were performed according to the manufacturer's recommendations (Sigma Aldrich). In brief, blots were blocked in PBS containing 2 % Tween for 2 min at 20 °C. Blots were then rinsed twice in PBS and incubated with 1 μg lectin-peroxidase ml^{-1} in PBS containing 0.05 % Tween, with 1 mM $CaCl_2$, 1 mM $MnCl_2$ and 1 mM $MgCl_2$, for 16 h at 20 °C. Surplus lectins were removed by rinsing with PBS; the blots were developed using the DAB staining kit with nickel enhancement (Vector Laboratories) (Linton *et al.*, 2002).

Microscopic examination. Atomic force microscopy (AFM) and transmission electron microscopy (TEM) were used to provide detailed visualizations of the surface morphology. AFM was carried out using W83 and FLL92 stains that were grown overnight to OD_{600} 1.2, washed twice in 0.1 M PBS buffer pH 7.4 and mounted on a cover slide. AFM was performed using the Innova Scanning Probe

Microscope (Veeco Instruments) in air, using the tapping mode. Images were captured in the height mode with a resolution of 256 × 256 (Pratto *et al.*, 2009). TEM was performed using the Philips Tecnai 12 TEM as per the method described by Harris (1991). Briefly, Formvar-carbon coated grids were prepared; the Formvar support was removed by placing the grids in an atmosphere of solvent vapour. Grids were then placed on a wire mesh in a glass Petri dish with carbon tetrachloride below the wire mesh. One microlitre of serially diluted sample was placed under the carbon side of a 4 × 5 mm square of mica (approx. twice the size of an electron microscope grid). The grid was washed in 0.5 % acetic acid then acetone. The carbon film was broken to free the specimen grid, after which the grid was placed in stain solution (neutral 1 % aqueous phosphotungstic acid) for 30 s. After blotting dry, the grid was examined using the Tecnai TEM (FEI).

Localization of FimA in *P. gingivalis* by immunogold staining. Anti-FimA antibodies (Lin *et al.*, 2006) were purified and used at a working concentration of 1 : 100. The colloidal gold conjugate (10 nm; Aurion) was diluted using incubation buffer (20 mM phosphate buffer, 150 mM NaCl pH 7.4, 0.2 % BSA, 15 mM NaN_3) to 1 : 1000. A checker board titration of primary antibody to immunogold conjugate was made to identify the optimal working concentration. Processed nickel grids were subjected to charging of the processed *P. gingivalis* strains for 1 h, then washed 20 times in 0.025 M Tris buffer (pH 7.4) and lightly blotted. Grids were subsequently blocked with 5 % BSA in 0.025 M Tris buffer for 15 min at room temperature, then incubated in diluted antibody–gold complex for 4 h at 37 °C. Staining was done using uranyl acetate (0.8 g uranyl acetate dissolved in 10 ml absolute ethanol) and freshly prepared lead citrate (10–40 mg lead citrate, 10 ml filtered water, 100 µl 10 M NaOH). Grids were immersed in uranyl acetate for 7 min at room temperature and then washed, once by immersion in 25 % ethanol and twice by immersion in water. Grids were dried on filter paper for 10 min at room temperature and then floated on lead citrate drops for 5 min. Following two washes by immersion in 0.02 M NaOH and drying, grids were visualized using the Philips Tecnai 12 TEM.

Hydrophobicity assay. Hydrophobicity assays of *P. gingivalis* strains were based on adhesion to hexadecane, as described by Grivet *et al.* (2000). Bacteria were harvested during exponential growth phase by centrifugation at 4 °C for 15 min, then they were washed with 0.1 M PBS (pH 7) and resuspended in PBS. The OD_{600} of the samples was adjusted to 0.85. Bacterial suspension (3 ml) was placed in a polystyrene tube to which 400 µl hexadecane was added. No hexadecane was added to the control suspensions. Suspensions were equilibrated in a water bath at 37 °C, vortexed for two 30 s periods with 5 s intervals and these were allowed to stand until the phases separated. The lower aqueous phase was carefully removed and its OD_{600} was determined. The values obtained were expressed as the percentage of bacteria remaining in the aqueous phase compared with the control suspension.

Determination of minimum inhibitory concentrations (MIC). Serial dilutions of antibiotics were used to determine MIC values in broth. These experiments were done in duplicate. In brief, broth macro dilutions of W83 and FLL92 were carried out using tubes containing 9 ml BHI-HK broth plus 1 ml of antibiotic dilution. Tubes were examined for turbidity after incubation at 37 °C for 72 h in an anaerobic chamber (Wright *et al.*, 1997). The MIC was taken as the concentration at which no visible growth was observed.

Labelling of *P. gingivalis* with [^{3}H]-palmitic acid. *P. gingivalis* cells were labelled according the protocol described by Shoji *et al.* (2004). Briefly, 5 ml cultures of W83 and FLL92 were incubated for 24 h in BHI-HK in the presence of 50 µCi palmitic acid [9,10(n)-^{3}H] ml^{-1} (MP Biomedicals). Cells were then centrifuged, washed in PBS buffer and homogenized using glass beads to derive total proteins. Protein fractions were subsequently separated on an SDS-PAGE gel. Radiolabelled proteins were detected using autoradiography as described by Voytas & Ke (2001).

Bioinformatic analysis of VimA. Protein modelling of VimA was conducted using I-Tasser (Zhang, 2008, 2009). The subcellular location of the protein was predicted from its amino acid sequence using SignalP 3.0 (Nielsen *et al.*, 1997), Phobius (Kall *et al.*, 2007) and PSORTb (Gardy *et al.*, 2005). Protein motifs and domains of VimA were identified using PPSearch (Pearson & Lipman, 1988) and Superfamily (Gough *et al.*, 2001).

Cell fractionation. The Sarkosyl method was used to prepare outer membrane fractions of *P. gingivalis* (Potempa *et al.*, 1995). In brief, *P. gingivalis* cells were harvested from a 500 ml culture during the exponential and stationary phase of the growth cycle (OD_{600} 0.6–1.0 and 1.5–1.8, respectively). Cells were pelleted at 9000 ***g*** for 30 min at 4 °C then resuspended in 5 ml 20 mM Tris/HCl (pH 7.4), 10 mM EDTA, 10 mM *N*-α-*p*-tosyl-L-lysine chloromethyl ketone (TLCK) and 1 % sodium lauryl sarcosinate. Cells were disrupted by passage through a French pressure cell at 109 MPa. Whole cells were removed by further centrifugation at 5000 ***g*** for 20 min at 4 °C. The outer membrane fraction was separated by centrifugation (100 000 ***g*** for 30 min), and then the pellet was washed three times in 0.5 % sodium lauryl sarcosinate and resuspended in 20 mM Tris/HCl (pH 7.4). Extracellular fractions were prepared from cell-free culture fluid precipitated with 60 % acetone (−20 °C) (Vanterpool *et al.*, 2006). The protein pellet was resuspended in 7 ml 100 mM Tris/HCl buffer (pH 7.4) in the presence of 1 mM TLCK, dialysed for 48 h against the same buffer, then stored at −20 °C. Total proteins were harvested from a 50 ml culture during the late exponential phase. Cells were pelleted at 8000 ***g*** for 30 min then resuspended in 1 ml 25 mM Tris/HCl (pH 8.0) with a protease inhibitor cocktail tablet (Complete EDTA-free, Roche), RNase and DNase (1 µg ml^{-1}). Resuspended cells were then transferred to a 2 ml cryogenic tube containing 1 g of 0.1 mm glass beads. Cells were lysed in a Beadbeater homogenizer for 4 min with 30 s intervals, with 1 min cooling on ice. Samples were then centrifuged (10 000 ***g***) for 12 min at 4 °C. The upper aqueous layer containing the total protein fraction was removed and stored on ice or at −20 °C.

Digestion of *P. gingivalis* wild-type and FLL92 proteins. Late exponential and stationary phase membrane proteins were separated on a 10 % Bis/Tris gel (Invitrogen) in 1 × MOPS running buffer for 1.5 cm, then visualized by staining with SimplyBlue safe stain (Invitrogen) (Henry *et al.*, 2008). After destaining in water, the gel was cut into 1–2 mm slices. Gel slices were subsequently dehydrated in acetonitrile and dried in a vacuum centrifuge for 30 min. The gel slices were incubated for 1 h at 60 °C in a solution containing 20 µl of 20 mM DTT in 100 mM NH_4HCO_3 (enough to cover the gel pieces). The DTT solution was replaced with an alkylating solution (20 µl of 200 mM iodoacetamide in 100 mM NH_4HCO_3) after cooling the proteins to room temperature. Gel slices were further incubated at ambient temperature for 30 min in the dark, followed by two washes with 150 µl of 100 mM NH_4HCO_3; the slices were then finely minced with a flame-sealed polypropylene pipette tip, dehydrated by the addition of acetonitrile and vacuum dried. Following an overnight incubation of the gel pieces with 20 µl digestion buffer [1 µl of mass spectrometry (MS)-grade trypsin (www.promega.com) in 50 mM acetic acid with 1 µl of 100 mM NH_4HCO_3], the digestion reaction was stopped with 10 µl of 5 % formic acid. After transferring the digest solution (aqueous extraction) to a 0.65 ml siliconized tube, 30 µl of 50 % acetonitrile with 0.1 % formic acid was added, the mixture was vortexed for 3 min, centrifuged and then sonicated for 5 min. The process was repeated and both extractions were pooled and concentrated to 10 µl in a vacuum centrifuge. Peptide extraction

was accomplished using standard C_{18} ZipTip technology following the manufacturer's directions (Millipore).

MS and data analysis. An LCQ Deca XP Plus system (www.thermo.com) with nano-electrospray technology (www.newobjective.com) consisting of a reverse-phase C_{18} separation of peptides on a 10 cm by 75 μm capillary column using Microm Magic RP-18AQ resin (www.michrom.com) with direct electrospray injection was used to analyse the extracted peptides from each gel piece (Henry *et al.*, 2008). A four part protocol was used for the MS and MS/MS analyses; this included one full MS analysis (from 450 to 1750 *m*/*z*) followed by three MS/MS events using data-dependent acquisition, where the most intense ion from a given full MS scan was subjected to collision-induced dissociation, followed by the second and third most intense ions. The nanoflow buffer gradient was extended over 45 min in conjunction with the cycle repeating itself every 2 s, using a 0–60 % acetonitrile gradient from buffer B (95 % acetonitrile with 0.1 % formic acid) developed against buffer A (2 % acetonitrile with 0.1 % formic acid) at a flow rate of 250–300 nl min^{-1}, with a final 5 min 80 % bump of buffer B before re-equilibration. In order to move the 20 μl sample from the autosampler to the nanospray unit, flow stream splitting (1 : 1000) and a Scivex 10 port automated valve (Upchurch Scientific) together with a Michrom nanotrap column was used. The spray voltage and current were set at 2.2 kV and 5.0 μA, with a capillary voltage of 25 V in positive ion mode. The spray temperature for peptides was 160 °C. Data collection was achieved using the Xcalibur software (Thermo Electron), then screened with Bioworks 3.1. MASCOT software (www.matrixscience.com) was used for each analysis to produce unfiltered data and output files. Statistical validation of peptide and protein findings was achieved using X! Tandem (www.thegpm.org) and SCAFFOLD 2 meta analysis software (www.proteomesoftware.com). The presence of two different peptides at a probability of at least 95 % was required for consideration of positive identification. Confirmation of individual peptide matches was achieved using the BLAST database (www.oralgen.lanl.gov).

RESULTS

In silico analysis of VimA reveals close similarity to the Fem family of proteins

Using I-Tasser, the putative structure of the VimA was modelled; this structure has a confidence score of 0.54 (Fig. 1a). Several binding sites were also predicted (Fig. 1b). The predicted structure is similar to the FemA of *Staphylococcus aureus* (TM-score 0.81) and FemX of *Weisella viridiscens* (TM-score 0.89). The gene ontology is predicted to include a role in one or more of the following: peptidoglycan biosynthetic process, cellular component biogenesis, cell wall biogenesis, peptidoglycan-based cell wall biogenesis, metabolic process, biosynthetic process, carbohydrate biosynthetic process, primary metabolic process, carbohydrate metabolic process and peptidoglycan metabolic process. SignalP 3.0 and PSORTb predicted no signal peptide in the VimA sequence, suggesting that this protein is not secreted. Phobius scored the likelihood of VimA being a non-cytoplasmic protein at 0.83. Using EMBL protein interaction software v.8.1, VimA was predicted to interact directly with several proteins, including several uncharacterized putative proteins of unknown functional aetiology. The cysteine proteases (PG0506-RgpB) were associated with VimA with a score of 0.808. The bacterioferritin combinatory protein had an interaction score of 0.582, meaning that it is involved in storage of iron in the form of hydrated ferric oxide. Lys1 mediates lysine biosynthesis through the enzyme saccharopine dehydrogenase, while RecA has multiple activities, all related to DNA repair. Position-specific iterative protein classifier and Superfam 3.0 predicted that VimA belongs to the DUF482/CH1444 and/or Acyl-CoA *N*-acyltransferase superfamily.

Surface morphology is affected by the *vimA* mutation

Auto-aggregation in *P. gingivalis* seems to be correlated with the absence of a capsule and the presence of fimbriae (Davey & Duncan, 2006). AFM and TEM were used to visualize potential differences between the mutant and the wild-type. Micrographs of W83 (Fig. 2a) and FLL92 (Fig. 2b) revealed differences in the capsular structure. The capsule of W83 was solid and well-defined in contrast with the capsule of FLL92, which was less defined and irregular. AFM micrographs of W83 (Fig. 2c) and FLL92

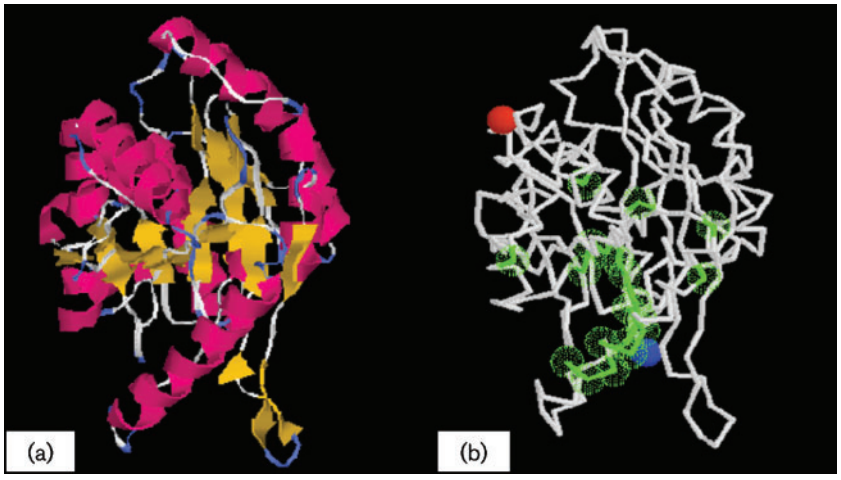

Fig. 1. (a) Model of the VimA protein (confidence score 0.54). The secondary structures are highlighted in red (α-helices) and yellow (β-strands). (b) Predicted binding site residues (green): Leu : 55 Gly : 56 Ser : 57, Phe : 71 Arg : 72 Ala : 73, Val : 77 His : 78 Met : 84, Tyr : 95 Ser : 96 Lys : 97, Tyr : 58 Ser : 59, Arg : 75 Arg : 76, His : 88 Phe : 91, and Gln : 108 Trp : 297. The N- and C-terminal residues are marked by blue and red spheres, respectively.

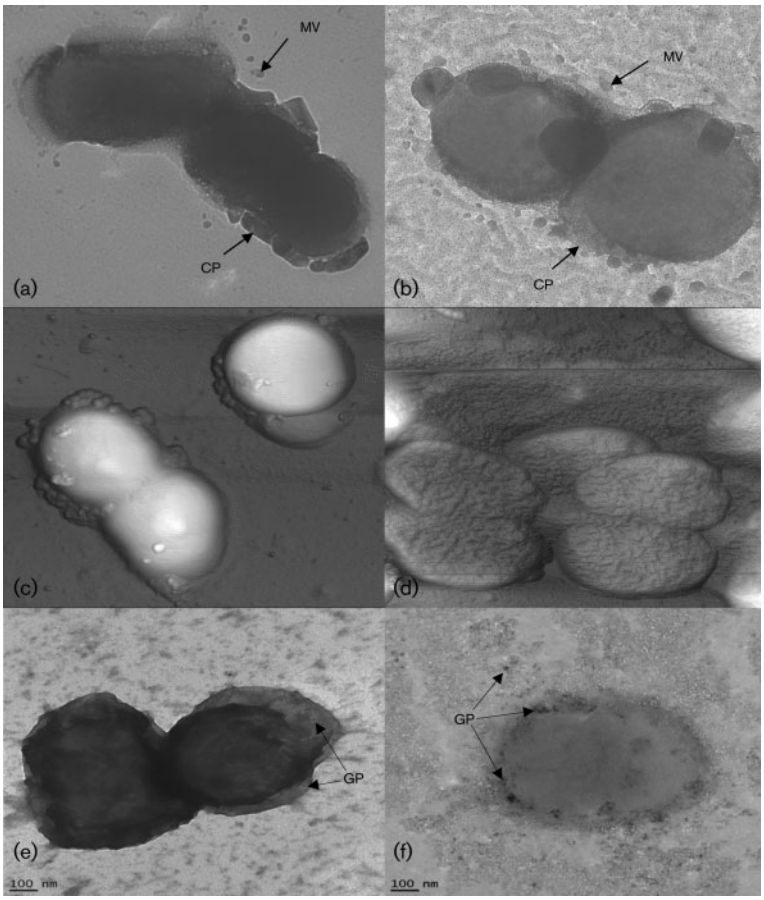

Fig. 2. TEM micrographs of W83 (a) and FLL92 (b) showing capsule (CP) with vesicles (MV). AFM micrographs of W83 (c) and FLL92 (d). Immunogold localization of *P. gingivalis* FimA in W83 (e) and FLL92 (f), visualized by TEM after incubation with anti-FimA serum conjugated to 10 nm gold particles (GP).

(Fig. 2d) showed that FLL92 had distinct fine structures, resulting in a corrugated appearance, in contrast with the smooth morphology of W83. FLL92 cells also tended to clump together. Immunogold staining of W83 (Fig. 2e) and FLL92 (Fig. 2f) showed adherence of gold particles to abundant fimbrial appendages in FLL92 in contrast with few gold particles adhering to W83.

Expression of fimbrial genes in the *vimA*-defective mutant

The autoaggregation observed in FLL92 could have been as a result of changes to the fimbrial protein. It is also possible that VimA may also be involved in the post-translational regulation of fimbrial expression. To confirm the presence of the mRNA transcript for the *fimA* gene, total RNA was isolated from wild-type and FLL92 strains grown to stationary phase. Using reverse transcriptase with specific oligonucleotide primers for an intragenic region of the *fimA* gene, a predicted 0.6 kb fragment was amplified for both the wild-type and FLL92 isogenic strain. Immunoblotting of outer membrane and total protein fractions of FLL92 and W83 with the FimA antibody revealed strong immunoreactivity with a 41–43 kDa band in both fractions of FLL92 (Fig. 3). This band, which corresponds with the expected size of FimA, was absent in both W83 fractions.

There is no change in the hydrophobicity or ability to form biofilm in FLL92

Adhesion to hexadecane was used to determine the hydrophobicity of W83 and FLL92; ATCC 33277 served as a control (known to form biofilm and to auto-aggregate). There was no change in the hydrophobicity

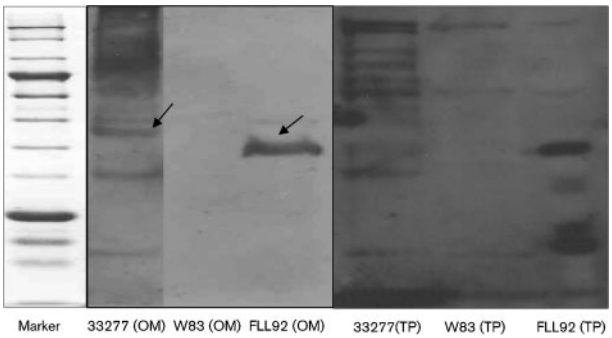

Fig. 3. Immunoblot analysis using anti-FimA antibody with outer membrane (OM) and total protein (TP) fractions of *P. gingivalis* ATCC 33277, W83 and FLL92. A 43 and 41 kDa protein corresponding with the expected size of FimA was observed in 33277 and in the *vimA* mutant, respectively (arrows).

profile of FLL92 compared with W83. Over half (55 %) of ATCC 33277 cells adhered to hexadecane; this reflects their hydrophilic surface properties. The ability of the *vimA*-defective mutant FLL92 to form biofilm, as quantified by adherence to the surface of 96-well plates, was unchanged when compared with W83 (data not shown).

Bacterial cell surface/membrane modifications can alter antimicrobial sensitivity

Several antibiotics with varying targets were employed in antibiotic sensitivity testing of FLL92. FLL92 showed increased sensitivity to globomycin (10 μg ml^{-1} compared with 25 μg ml^{-1} in W83) and vancomycin (5 μg ml^{-1} compared with 10 μg ml^{-1} in W83).

VimA affects outer-membrane proteins glycosylated with specific carbohydrate moieties

Previous reports from our laboratory have documented the changes in the glycosylation profile of FLL92 compared with wild-type W83 (Vanterpool *et al.*, 2005b). To further confirm the role of VimA in post-translational glycosylation of outer-membrane proteins, lectins were used. Differential lectin-bound protein profiles were observed using ConA, DBA, ECA, LPA and SBA (Fig. 4). No discernible differences were observed using WGA or ABA.

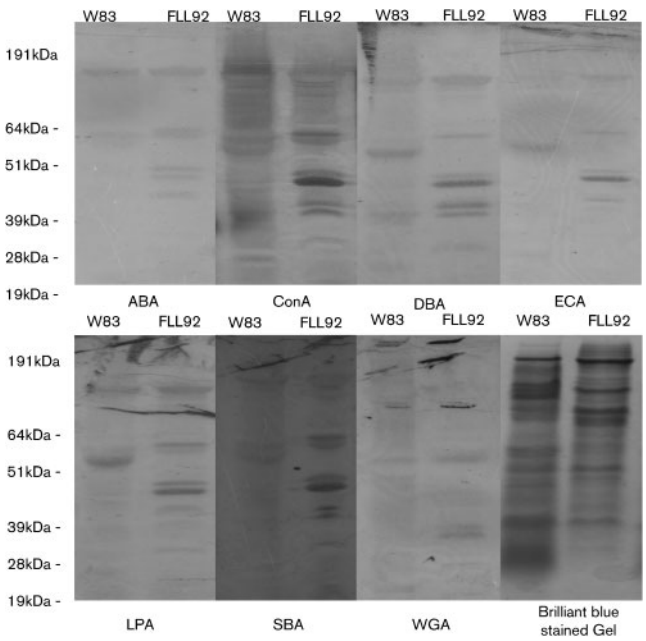

Fig. 4. Outer-membrane preparations from *P. gingivalis* W83 and FLL92 were separated by SDS-PAGE, transferred to nitrocellulose membranes, blocked in PBS then incubated with lectin-peroxidase overnight. Peroxidase activity was detected using the DAB peroxidase substrate kit. Differential lectin binding was observed using ABA, ConA, DBA, ECA, LPA, SBA and SGA.

VimA affects the anchorage of several membrane-bound proteins

MS analysis of membrane fractions of W83 and FLL92 identified 20 proteins that were absent from the wild-type membrane fraction but present in the FLL92 fraction (Table 1). While 13 of these proteins are hypothetical, PG0083, PG0581, PG0602, PG0703 and PG1496 are predicted to be involved in transport (www.oralgen.lanl.gov). Nine proteins were identified as missing from the FLL92 fraction compared with the wild-type (Table 2). These included three proteases – RgpA (PG1768), Kgp (PG1605) and carboxypeptidase D (PG0212) – in addition to PG0554 and PG1136, which are predicted to be involved in amino acid biosynthesis (www.oralgen.lanl.gov). PG1857, which is predicted to be involved glycolysis or gluconeogenesis (www.oralgen.lanl.gov), was also missing. Twenty-one membrane proteins were identified as having variable spectral counts (Table 3), corresponding with a fold change of 1.4 or greater. Ten of these proteins showed a positive fold change in the *vimA* mutant, while 11 showed a negative fold change. The majority of these proteins were predicted to be involved in cell envelope biogenesis or transport (www.oralgen.lanl.gov).

Analysis of missing membrane proteins reveals several common motifs

Using PPSearch (www.ebi.ac.uk/Tools/ppsearch), several common domains were identified in the missing proteins identified by MS analysis (Table 4). In PG1768 (RgpA), PG1605 (Kgp), PG0212 (carboxypeptidase D) and PG0981 (hypothetical), the most abundant motifs were myristoylation sites (13, 11, 49 and 37, respectively), casein kinase II phosphorylation motifs (19, 14, 29 and 35, respectively) and protein kinase C motifs (15, 16, 27 and 20, respectively).

Palmitic acid assay shows that VimA is involved in the acylation of proteins

Several outer-membrane proteins are lipid-modified in *P. gingivalis* (Yoshimura *et al.*, 2009). To determine whether VimA could play a role in lipid modification of proteins, *P. gingivalis* was grown in the presence of ^{3}H-labelled palmitic acid. No change in the acylation profile was observed in the total protein fractions of the wild-type or FLL92 grown to exponential phase (Fig. 5b). In the extracellular fraction from FLL92 grown to exponential phase (Fig. 5b), a 54 kDa protein was observed in W83 which had three times the intensity of that observed in FLL92; while a 27 kDa protein was observed in FLL92 with twice the intensity of W83 (Fig. 5c).

DISCUSSION

Membrane integrity is critical to the survival, adaptability and pathogenicity of bacteria (Duban *et al.*, 1993; Frirdich

Table 1. MS analysis of aberrantly expressed proteins in FLL92

The spectral count value (SCV) for W83 was 0 for all proteins.

Identified protein	GenBank accession no.	Putative role/function	Molecular weight (kDa)	FLL92 SCV
Conserved hypothetical protein (possible alkaline secretion protease)	PG0083	Transport and binding	56	4
Conserved hypothetical protein (possible lipoprotein)	PG0219	Unknown	32	82
Hypothetical protein	PG0302	Unknown	47	7
Conserved hypothetical protein	PG0332	Unknown	22	1
Hypothetical protein	PG0334	Unknown	82	2
Conserved hypothetical protein	PG0373	Unknown	30	16
Conserved hypothetical protein	PG0410	Unknown	48	4
Periplasmic serine protease	PG0535	Proteolysis	53	1
TonB receptor tlr (C-terminal part)	PG0581	Transport	44	4
Haem-binding protein/peripheral outer membrane chelatase	PG0602	Transport and binding	33	4
Probable biopolymer transport (TolQ) protein	PG0703	Transport	29	3
Hypothetical protein	PG0809	Unknown	16	2
Conserved hypothetical protein	PG0922	Unknown	55	7
Probable outer membrane lipoprotein	PG1177	Cell wall biogenesis	21	18
Conserved hypothetical protein	PG1308	Unknown	100	24
Conserved hypothetical protein	PG1496	Transport	99	19
Conserved hypothetical protein	PG1772	Proteolysis	98	4
Hypothetical protein	PG1790	Unknown	10	1
Outer-membrane protein (immunogenic 23 kDa lipoprotein)	PG1793	Cell wall biogenesis	23	44
Probable integral outer-membrane protein	PG1840	Cell wall biogenesis	24	24

& Whitfield, 2005; Zaas *et al.*, 2005). In this study, we examined the role of VimA on membrane proteins and structures, with a view to further elucidate its role in modulating virulence in *P. gingivalis*. The role of VimA in gingipain maturation, auto-aggregation, haemolysis, haemagglutination and LPS synthesis has been alluded to in previous reports (Vanterpool *et al.*, 2004, 2005a, b, 2006); however, its role in membrane biogenesis has not been explored. The unique phenotype of FLL92 led us to hypothesize that VimA plays a significant role in membrane biogenesis of *P. gingivalis* and is integral for anchorage and maturation of membrane proteins.

In silico analysis of the VimA protein predicted a structure that showed similarity to the Fem family of proteins. These proteins are found in Gram-positive bacteria and are involved in cell envelope biogenesis, particularly in peptidoglycan formation (Brakstad & Maeland, 1997; Mainardi *et al.*, 2008; Stapleton & Taylor, 2002). Interestingly, this protein is not predicted to be involved in secretion or cytoplasmic localization, suggesting that it is likely a transmembrane or periplasmic protein. Attempts to localize this protein with antibodies raised against the overexpressed protein in *Escherichia coli* have so far proven unsuccessful. The VimA protein could be classified in the

Table 2. MS analysis of missing proteins in FLL92

The spectral count value (SCV) for FLL92 was 0 for all proteins.

Identified protein	GenBank accession no.	Putative role/function	Molecular weight (kDa)	W83 SCV
Carboxypeptidase D/immunoreactive 92 kDa antigen	PG0212	Proteolysis	92	3
Hypothetical protein	PG0554	Cell redox homeostasis	38	95
Conserved hypothetical protein	PG0981	Unknown	107	3
Branched-chain amino acid aminotransferase	PG1136	Amino acid biosynthesis	38	11
Peptidylarginine deiminase	PG1249	Arginine and proline metabolism	62	100
Porphypain polyprotein; lys-X proteinase/ haemagglutinin	PG1605	Proteolysis/pathogenesis/DNA replication and repair	188	60
Hypothetical protein	PG1722.1	Unknown	24	5
Arginine-specific cysteine proteinase; gingipain	PG1768	Proteolysis/pathogenesis/DNA replication and repair	186	92
Glyceraldehyde 3-phosphate dehydrogenase	PG1857	Glycolysis/gluconeogenesis	36	60

Table 3. MS analysis of proteins with different spectral count values in W83 and FLL92

Identified protein	GenBank accession no.	Putative role/ involvement	Molecular weight (kDa)	Fold change	W83 SCV	FLL92 SCV
Probable outer membrane lipoprotein	PG0916	Cell envelope	63	7.1	26	185
Possible outer membrane-associated protein	PG1893	Cell envelope	54	4.0	40	10
TonB-linked outer membrane receptor	PG0601	Transport and binding	85	3.6	5	18
Possible outer membrane-associated protein	PG1424	Cell envelope	61	3.2	17	54
Outer-membrane protein	PG0626	Cell envelope	42	2.6	156	408
Possible lipoprotein	PG1600	Unknown	51	2.2	5	11
Outer-membrane protein	PG0627	Cell envelope	43	2.0	129	256
Probable integral outer-membrane protein	PG1592	Cell envelope	24	1.9	29	56
Probable integral outer-membrane protein	PG1562	Cell envelope	32	1.6	11	17
TonB-dependent outer membrane receptor	PG0170	Transport	112	1.5	452	674
Receptor antigen B	PG0171	Cell envelope	56	−1.4	455	316
TonB-linked receptor tlr	PG0582	Transport	51	−1.4	14	10
TonB-linked outer membrane receptor	PG1752	Transport	93	−1.5	15	10
Hypothetical protein	PG0197	Unknown	33	−1.8	9	5
Conserved hypothetical protein; possible TonB-dependent receptor	PG0899	Transport	100	−2.0	8	4
Outer-membrane protein, TonB-dependent receptor	PG0637	Transport	94	−2.9	52	18
Phenylalanine/histidine ammonia-lyase	PG0299	Histidine catabolysis	55	−3.3	23	7
Outer-membrane protein	PG1901	Cell envelope	32	−3.6	29	8
β-Galactosidase	PG0598	Carbohydrate metabolism	127	−3.8	15	4
Hypothetical protein	PG1894	Unknown	21	−10.8	43	4

DUF482/CH1444 and/or acyl-CoA *N*-acyltransferase superfamily. DUF482/CH1444 is part of the PEP-CTERM system that has sortase-like function and is involved in bacterial exopolysaccharide biosynthesis (Haft *et al.*, 2006). Proteins exported in this system have conserved C-terminal sorting signals that are recognized by a sortase in Gram-

Table 4. Number of predicted motifs present in missing FLL92 membrane proteins

	PG0212*	PG0554	PG0981	PG1136	PG1249	PG1605	PG1722.1	PG1768	PG1857
MYR†	13	3	11	6	8	49	7	37	7
TYR_PHOS‡	0	0	2	0	0	1	0	0	0
CK2_PHOS§	19	5	14	4	5	29	3	25	8
PKC_PHOS‖	15	5	16	3	6	27	5	20	5
CAMP_PHOS¶	1	0	1	0	1	2	1	2	1
ASN_GLYC#	8	4	0	3	5	15	1	17	3
Amidation**	1	0	3	0	1	4	0	4	0
Unique	Zinc_Car††	None	None	None	None	DNA-Lig‡‡	None	DNA-Lig	GAPDH§§

*Each protein's GenBank accession number is given in the table; see Table 2 for details of the proteins.
†*N*-Myristoylation site.
‡Tyrosine kinase phosphorylation site.
§Casein kinase II phosphorylation site.
‖Protein kinase C phosphorylation site.
¶cAMP- and cGMP-dependent protein kinase phosphorylation site.
#*N*-Glycosylation site.
**Amidation site.
††Zinc carboxypeptidase.
‡‡ATP-dependent DNA ligase AMP-binding site.
§§GAPDH active site.

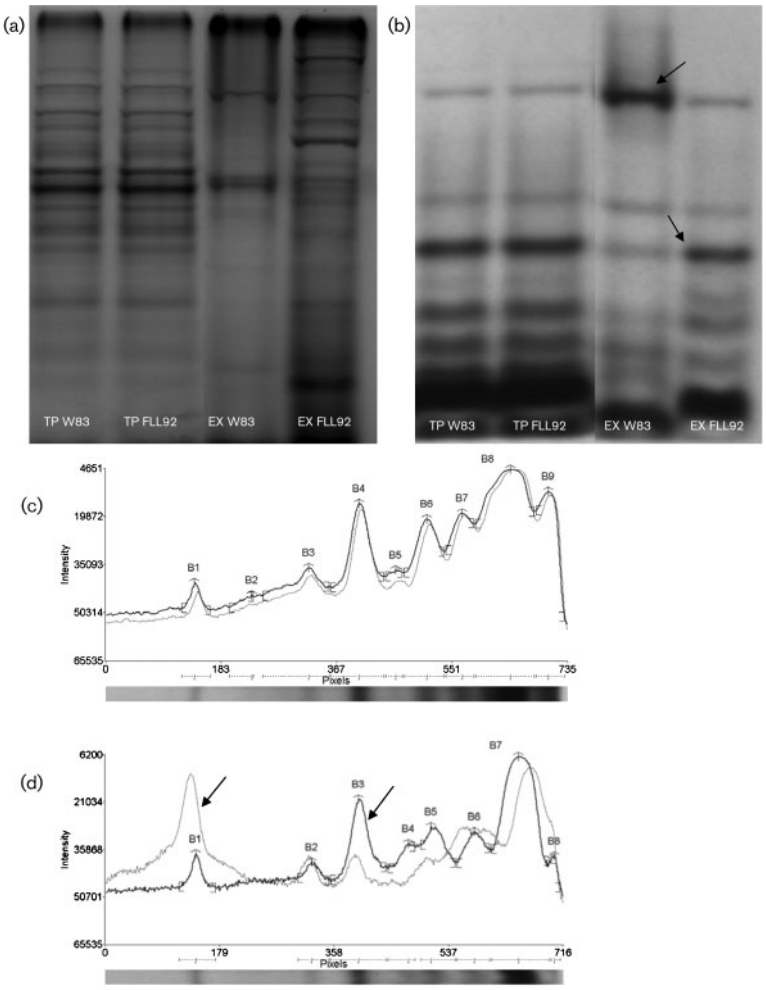

Fig. 5. Autoradiography of total protein (TP) and extracellular fractions (EX) of W83 and FLL92 grown overnight in the presence of ^{3}H-labelled palmitic acid. (a, b) Brilliant blue-stained SDS-PAGE gel (a) and ^{3}H-labelled palmitic acid nitrocellulose membrane (b) with W83 and FLL92 TP and EX fractions. (c, d) Densitometric analysis of ^{3}H lipid-labelled proteins of W83 (grey) and FLL92 (black) total protein (c) and extracellular (d) fractions. A 54 kDa protein (B1) was three times as abundant in W83 compared with FLL92 and the 27 kDa protein (B3) was twice as abundant in FLL92 compared with W83 (see arrows).

positive bacteria (Desvaux *et al.*, 2006; Dramsi *et al.*, 2005; Marraffini *et al.*, 2006; Ton-That *et al.*, 2004; Tsukiji & Nagamune, 2009) or an analogous system termed exosortase in Gram-negative bacteria (Salinero *et al.*, 2009). The second predicted family (acyl-CoA *N*-acyltransferase) is a broad family which includes *N*-acetyltransferase, *N*-myristoyl transferase, autoinducer synthase, FemXAB nonribosomal peptidyltransferases, ornithine decarboxylase antizyme-like, AstA-like, DUF1122 and EF1021-like subfamilies. VimA is predicted to belong to the FemXAB nonribosomal peptidyltransferase subfamily. Notably, VimA is predicted to interact with RgpB (score 0.81) in addition to several other proteins; this is consistent with previous reports which demonstrate that VimA is able to interact with RgpB. Interestingly, several proteins, including those coded for upstream and downstream of *vimA*, are predicted to interact with VimA, and it is noteworthy that several proteins, including PG1605 (Kgp), PG0010 (*β*-lactamase), PG1101 (alanyl-tRNA synthase), PG0535 (HtrA), PG1833 (RegT), PG0324 (putative sialidase) and PG1768 (RgpA), that have been previously shown to interact (Vanterpool *et al.*, 2006) were not predicted for interaction with Vim A. These data suggest that VimA is likely to be a multifunctional protein, possibly forming a complex with those proteins encoded at the *recA* locus, and may modulate several virulence factors in addition to being involved in the biosynthesis of membrane proteins and structures.

We have demonstrated in previous studies that compared with the wild-type, FLL92 autoaggregates (Olango *et al.*, 2003). Several reports have suggested that the expression of fimbriae and the absence of a capsule may contribute to auto-aggregation, which in turn increases the organism's ability to form biofilm (Davey & Duncan, 2006). Visible differences were observed between FLL92 and W83. These differences related to capsular formation and surface morphology. The capsule of FLL92 was irregular and fuzzy in contrast with the solid defined capsule of W83. FLL92 also had a corrugated surface morphology compared with the smooth morphology present in W83. Abundant immunogold particles were observed in the appendage-like structures of FLL92; however, few gold particles were incorporated in the few surface-related appendages of W83. Interestingly, RT-PCR demonstrated that the *fimA* gene was similarly expressed in both the wild-type and *vimA*-defective isogenic mutant.

The presence of major fimbriae in wild-type W83 was previously disputed (Nishiyama *et al.*, 2007), as screening by immunological means such as bacterial agglutination, ouchterlony immunodiffusion and Western blotting were all negative; however, electron microscopy has been used successfully to establish that W83 is poorly fimbriated (Handley & Tipler, 1986; Suzuki *et al.*, 1988). This is in contrast with highly fimbriated strains such as 33277 and 381 which show positive immunological fimbrial results and positive visualization by electron microscopy. In *P. gingivalis*, there are six classifications of the *fimA* gene (I, Ib, II, III, IV and V) (Amano *et al.*, 2004); the large majority of patients carry either type II or IV *fimA*. Interestingly, these genotypic differences do not correlate with morphological differences in fimbriae (Amano *et al.*, 2000). W83 is type IV, whereas 33277 and 381 are type I (Nishiyama *et al.*, 2007). The relationship between capsular and fimbrial synthesis is at present unknown in *P. gingivalis*; however, as has been demonstrated in *Klebsiella pneumoniae* (Matatov *et al.*, 1999; Sahly *et al.*, 2000), fimbrial function can be impeded by expression of the polysaccharide capsule and can be restored by inhibiting capsular synthesis. Capsular formation may also impede assembly of preformed fimbrial subunits on the bacterial surface (Sahly *et al.*, 2000). This effect in *K. pneumoniae* is due to direct physical interaction as opposed to transcriptional or translational changes, and is in keeping with our own observations which show that the *fimA* transcript is made in the wild-type and the mutant. Therefore, in light of the effect of the *vimA* mutation on capsular synthesis, fimbrial function and synthesis may no longer be impeded, resulting in the assembly of fimbriae on the surface. The presence of the *fimA* message coupled with undetected FimA via immunoblotting, may also indicate a role for *vimA* in protein synthesis and turnover. Interestingly, these alterations in membrane structure did not affect the organism's ability to form biofilm. Taken together, these findings indicate a critical role for VimA in capsular biogenesis and probably an indirect role in fimbrial synthesis. Further studies are actively being pursued in our laboratory to elucidate the role of VimA in synthesis and regulation of the capsule and fimbriae.

The corrugated surface morphology of FLL92 coupled with previous reports which demonstrated that although there are more proteins present in the membrane fraction, other proteins such as RgpA and Kgp are missing (Vanterpool *et al.*, 2005b, 2006), could suggest that this morphology was likely due to the aberrant anchorage and/or expression of proteins on the cell membrane. Our findings revealed 20 proteins that were aberrantly anchored to the cell wall of FLL92, 9 proteins that were missing and 21 proteins which had variable spectral count values. These normalized spectral count values correlate to the relative abundance of these proteins. Of the nine missing proteins; three are involved in proteolysis; these include carboxypeptidase D (PG0212), RgpA (1768) and Kgp (1605). GAPDH (PG1857) and peptidyl–arginine deiminase (PG1249) were also missing.

RgpA and Kgp proteinases and adhesins are C-terminally processed by carboxypeptidase D, otherwise known as carboxypeptidase CPG70. This protein shares C-terminal sequence similarity to cysteine proteinases, indicating a common mechanism for cell surface attachment and secretion (Chen *et al.*, 2002; Veith *et al.*, 2004). The absence of this carboxypeptidase on the surface of FLL92 likely explains why RgpA and Kgp are incorrectly modified and inactive, existing in the extracellular milieu, but not anchored to the surface. This is in contrast with the surface-bound yet inactive RgpB. GAPDH is a metabolic enzyme of the glycolytic pathway which phosphorylates glyceraldehyde-3-phosphate to generate 1,3 biphosphoglycerate (Lama *et al.*, 2009). GAPDH has also been shown to exist on the surface of bacterial pathogens, functioning as a novel virulence factor in several bacterial species by binding host proteins (Maeda *et al.*, 2004; Pancholi & Fischetti, 1992). In *Trichomonas vaginalis*, this enzyme binds fibronectin, plasminogen and collagen (Lama *et al.*, 2009), while in enterohaemorrhagic *E. coli* and enteropathogenic *E. coli*, it binds human plasminogen and fibrinogen (Egea *et al.*, 2007). In *Candida albicans*, this surface-associated enzyme binds to laminin and fibronectin (Gozalbo *et al.*, 1998). Surface-bound GADPH of *Streptococcus oralis* has been shown to play a role in *P. gingivalis* colonization. FimA of *P. gingivalis* is able to bind to GADPH present on the streptococcal surface (Nagata *et al.*, 2009); this interaction is further used to bind to human oral epithelial cells (Kinoshita *et al.*, 2008). The function of surface-bound GADPH in *P. gingivalis* has not been elucidated; however, we speculate that it is probably serving to bind host extracellular matrix proteins present within the periodontal pocket for proteolytic degradation by the gingipains. It is also possible that this protein may itself contain a binding receptor for other oral bacteria so as to allow for biofilm formation and colonization of the oral cavity. Peptidyl arginine deiminase (PAD), which catalyses the deimination of the guanidino group from carboxy-terminal Arg residues to produce ammonia, is released by *P. gingivalis*, which leads to the progression and development of adult-onset periodontitis. By producing ammonia, PAD provides a protective effect to the bacterium during the acid cleansing cycles of the mouth (Shirai *et al.*, 2001). The activity of PAD among cells, supernatant and vesicles is growth dependent. It has also been suggested that the interaction between PAD and Arg-X may arise from Arg-X cleaving anti-adhesive humoral defence peptides containing internal arginyl residues and other arginine carboxyl terminal defence peptides, which are then inactivated by PAD (McGraw *et al.*, 1999; Rodriguez *et al.*, 2009). It is likely that anchorage of PAD may be dependent on the carboxypeptidase D processing. The reported interaction between Arg-X and PAD leads us to hypothesize that the enzymic capabilities of PAD may be compromised as Arg-X is inactive, thus reducing its efficacy. Further studies are needed to clarify this hypothesis.

When missing proteins were examined for protein motifs using PPsearch, a protein motif identification software,

myristoylation and phosphorylation sites were in great abundance in all of the missing proteins. Of the 20 proteins, 13 were hypothetical proteins, 9 of which had an unknown function. Further, PG0535 (serine periplasmic protein), which has been shown to interact with VimA, is aberrantly expressed on the membrane of FLL92. This study also confirmed the missing membrane-associated RgpA and Kgp in FLL92, as previously reported (Vanterpool *et al.*, 2005b, 2006). These findings potentially explain the auto-aggregation that is observed in FLL92 and support a role for VimA in anchorage and maturation of membrane proteins, possibly through myristoylation or phosphorylation. The specific interaction between VimA and missing or aberrantly expressed proteins is being investigated.

In the *vimA*-defective mutant, there is aberrant protein glycosylation (Vanterpool *et al.*, 2005b). It is not known, however, whether this aberrant glycosylation is specific to certain carbohydrate moieties. To clarify the effect of the *vimA* mutation on glycosylation of outer-membrane proteins, lectins were used. Outer-membrane proteins glycosylated with galactose (β 1,3) *N*-acetylgalactosamine, *N*-acetyl-α-D-galactosamine, galactose (β 1,4) *N*-acetylglucosamine, *N*-acetyl-D-galactosamine and sialic acid (*N*-acetyl neuramic acid) were affected by the *vimA* mutation. We are still actively exploring whether this is due to the glycosylation of aberrantly expressed proteins (i.e. proteins that are not present on the wild-type membrane but are present on the membrane of FLL92) or proteins that are incorrectly processed, as is the case with RgpB. These findings suggest that VimA plays a role in the correct glycosylation of several membrane proteins.

Since several outer-membrane proteins are lipid-modified in *P. gingivalis* (Slakeski *et al.*, 2002), and in keeping with the likely role of the VimA protein as a possible acyl transferase, we incubated W83 and FLL92 with ^{3}H-labelled palmitic acid (lipid donor). The expression profile of lipid-modified proteins in the wild-type and mutant was unchanged. This suggests either that VimA is not involved in the acylation of outer-membrane proteins or that there is a redundant mechanism of protein acylation. To this end, PG1355 (putative acyltransferase) was upregulated (3.5-fold change) in FLL92 (unpublished microarray data) compared with the mutant. Interestingly, densitometric analysis of the extracellular fractions of W83 and FLL92 for lipid-modified proteins revealed a 54 kDa protein that was three times more abundant in W83 than was observed in FLL92. We also observed a 27 kDa protein that was twice as abundant in FLL92 as in W83. The above findings may indicate a likely role for VimA in the proper acylation of a 54 kDa extracellular protein; however, we have not ruled out the possibility that this protein is a dimer of the 27 kDa protein observed in the extracellular fraction of FLL92. Several reports have demonstrated that acylation is important for protein folding and protein–protein interaction, as well as ligand-induced conformational changes (Athavankar & Peterson, 2003; Herlax *et al.*, 2009; Olsen & Kaarsholm, 2000). It is possible that correct acylation of the 27 kDa extracellular protein leads to dimerization. In the *vimA* mutant, aberrant acylation of the 27 kDa extracellular protein may occur, resulting in higher levels of monomeric protein form. Further studies in our laboratory are seeking to clarify this position.

The expression of additional proteins attributed to membrane biosynthesis and transport in the VimA mutant suggest that several post-translational modification pathways may be affected by this protein. These modifications could include myristoylation and glycosylation. Co-translational modifications of proteins could be attributed to their involvement in signal transduction pathways as molecular switches associated with glycine-rich protein motifs. Myristoylation of proteins is reported to be involved in the type III secretory system in prokaryotes (Nimchuk *et al.*, 2000)

The missing and aberrantly expressed proteins in FLL92 suggest that VimA could have sorting/transport functions. VimA could also function as an acyl-CoA *N*-acyltransferase enzyme involved in protein modification or anchorage of membrane proteins. In conclusion, our results highlight a putative central role for VimA in protein modification and transport, possibly triggering cascade reactions that may modulate the virulence potential of *P. gingivalis*. The putative multiple functions of VimA need further clarification.

ACKNOWLEDGEMENTS

This work was supported by Loma Linda University and Public Health Grant DE13664 and DE019730 from NIDCR (to H. M. F.). We thank Professor Masatoshi Inukai for the globomycin antibiotic, Dr Hua Xie for the FimA antibody and Dr Danielo Boskovic for helpful comments concerning the acylation studies.

REFERENCES

Abaibou, H., Chen, Z., Olango, G. J., Liu, Y., Edwards, J. & Fletcher, H. M. (2001). *vimA* gene downstream of *recA* is involved in virulence modulation in *Porphyromonas gingivalis* W83. *Infect Immun* **69**, 325–335.

Amano, A., Nakagawa, I., Kataoka, K., Morisaki, I. & Hamada, S. (1999). Distribution of *Porphyromonas gingivalis* strains with *fimA* genotypes in periodontitis patients. *J Clin Microbiol* **37**, 1426–1430.

Amano, A., Kuboniwa, M., Nakagawa, I., Akiyama, S., Morisaki, I. & Hamada, S. (2000). Prevalence of specific genotypes of *Porphyromonas gingivalis fimA* and periodontal health status. *J Dent Res* **79**, 1664–1668.

Amano, A., Nakagawa, I., Okahashi, N. & Hamada, N. (2004). Variations of *Porphyromonas gingivalis* fimbriae in relation to microbial pathogenesis. *J Periodontal Res* **39**, 136–142.

Athavankar, S. & Peterson, B. R. (2003). Control of gene expression with small molecules: biotin-mediated acylation of targeted lysine residues in recombinant yeast. *Chem Biol* **10**, 1245–1253.

Bogen, G. & Slots, J. (1999). Black-pigmented anaerobic rods in closed periapical lesions. *Int Endod J* **32**, 204–210.

Brakstad, O. G. & Maeland, J. A. (1997). Mechanisms of methicillin resistance in staphylococci. *APMIS* **105**, 264–276.

Chen, Y. Y., Cross, K. J., Paolini, R. A., Fielding, J. E., Slakeski, N. & Reynolds, E. C. (2002). CPG70 is a novel basic metallocarboxypeptidase with C-terminal polycystic kidney disease domains from *Porphyromonas gingivalis*. *J Biol Chem* **277**, 23433–23440.

Cutler, C. W., Kalmar, J. R. & Genco, C. A. (1995). Pathogenic strategies of the oral anaerobe, *Porphyromonas gingivalis*. *Trends Microbiol* **3**, 45–51.

Dave, S. & Van, D. T. (2008). The link between periodontal disease and cardiovascular disease is probably inflammation. *Oral Dis* **14**, 95–101.

Davey, M. E. & Duncan, M. J. (2006). Enhanced biofilm formation and loss of capsule synthesis: deletion of a putative glycosyltransferase in *Porphyromonas gingivalis*. *J Bacteriol* **188**, 5510–5523.

Demmer, R. T. & Desvarieux, M. (2006). Periodontal infections and cardiovascular disease: the heart of the matter. *J Am Dent Assoc* **137** (Suppl.), 14S–20S.

Desvaux, M., Dumas, E., Chafsey, I. & Hebraud, M. (2006). Protein cell surface display in Gram-positive bacteria: from single protein to macromolecular protein structure. *FEMS Microbiol Lett* **256**, 1–15.

Dramsi, S., Trieu-Cuot, P. & Bierne, H. (2005). Sorting sortases: a nomenclature proposal for the various sortases of Gram-positive bacteria. *Res Microbiol* **156**, 289–297.

Duban, M. E., Lee, K. & Lynn, D. G. (1993). Strategies in pathogenesis: mechanistic specificity in the detection of generic signals. *Mol Microbiol* **7**, 637–645.

Egea, L., Aguilera, L., Gimenez, R., Sorolla, M. A., Aguilar, J., Badia, J. & Baldoma, L. (2007). Role of secreted glyceraldehyde-3-phosphate dehydrogenase in the infection mechanism of enterohemorrhagic and enteropathogenic *Escherichia coli*: interaction of the extracellular enzyme with human plasminogen and fibrinogen. *Int J Biochem Cell Biol* **39**, 1190–1203.

Ford, P. J., Yamazaki, K. & Seymour, G. J. (2007). Cardiovascular and oral disease interactions: what is the evidence? *Prim Dent Care* **14**, 59–66.

Frirdich, E. & Whitfield, C. (2005). Lipopolysaccharide inner core oligosaccharide structure and outer membrane stability in human pathogens belonging to the *Enterobacteriaceae*. *J Endotoxin Res* **11**, 133–144.

Gardy, J. L., Laird, M. R., Chen, F., Rey, S., Walsh, C. J., Ester, M. & Brinkman, F. S. (2005). PSORTb v.2.0: expanded prediction of bacterial protein subcellular localization and insights gained from comparative proteome analysis. *Bioinformatics* **21**, 617–623.

Gough, J., Karplus, K., Hughey, R. & Chothia, C. (2001). Assignment of homology to genome sequences using a library of hidden Markov models that represent all proteins of known structure. *J Mol Biol* **313**, 903–919.

Gozalbo, D., Gil-Navarro, I., Azorin, I., Renau-Piqueras, J., Martinez, J. P. & Gil, M. L. (1998). The cell wall-associated glyceraldehyde-3-phosphate dehydrogenase of *Candida albicans* is also a fibronectin and laminin binding protein. *Infect Immun* **66**, 2052–2059.

Grivet, M., Morrier, J. J., Benay, G. & Barsotti, O. (2000). Effect of hydrophobicity on *in vitro* streptococcal adhesion to dental alloys. *J Mater Sci Mater Med* **11**, 637–642.

Haft, D. H., Paulsen, I. T., Ward, N. & Selengut, J. D. (2006). Exopolysaccharide-associated protein sorting in environmental organisms: the PEP-CTERM/EpsH system. Application of a novel phylogenetic profiling heuristic. *BMC Biol* **4**, 29.

Handley, P. S. & Tipler, L. S. (1986). An electron microscope survey of the surface structures and hydrophobicity of oral and non-oral species of the bacterial genus *Bacteroides*. *Arch Oral Biol* **31**, 325–335.

Harris, J. R. (1991). *Electron Microscopy in Biology: a Practical Approach*. Oxford, UK: IRL Press.

Henry, L. G., Sandberg, L., Zhang, K. & Fletcher, H. M. (2008). DNA repair of 8-oxo-7,8-dihydroguanine lesions in *Porphyromonas gingivalis*. *J Bacteriol* **190**, 7985–7993.

Herlax, V., Mate, S., Rimoldi, O. & Bakas, L. (2009). Relevance of fatty acid covalently bound to *Escherichia coli* α-hemolysin and membrane microdomains in the oligomerization process. *J Biol Chem* **284**, 25199–25210.

Imamura, T. (2003). The role of gingipains in the pathogenesis of periodontal disease. *J Periodontol* **74**, 111–118.

Kall, L., Krogh, A. & Sonnhammer, E. L. (2007). Advantages of combined transmembrane topology and signal peptide prediction – the Phobius web server. *Nucleic Acids Res* **35**, W429–W432.

Kato, T., Tsuda, T., Omori, H., Kato, T., Yoshimori, T. & Amano, A. (2007). Maturation of fimbria precursor protein by exogenous gingipains in *Porphyromonas gingivalis* gingipain-null mutant. *FEMS Microbiol Lett* **273**, 96–102.

Kinoshita, H., Wakahara, N., Watanabe, M., Kawasaki, T., Matsuo, H., Kawai, Y., Kitazawa, H., Ohnuma, S., Miura, K. & other authors (2008). Cell surface glyceraldehyde-3-phosphate dehydrogenase (GAPDH) of *Lactobacillus plantarum* LA 318 recognizes human A and B blood group antigens. *Res Microbiol* **159**, 685–691.

Kumada, H., Haishima, Y., Umemoto, T. & Tanamoto, K. (1995). Structural study on the free lipid A isolated from lipopolysaccharide of *Porphyromonas gingivalis*. *J Bacteriol* **177**, 2098–2106.

Kuramitsu, H. K. (1998). Proteases of *Porphyromonas gingivalis*: what don't they do? *Oral Microbiol Immunol* **13**, 263–270.

Lama, A., Kucknoor, A., Mundodi, V. & Alderete, J. F. (2009). Glyceraldehyde-3-phosphate dehydrogenase is a surface-associated, fibronectin-binding protein of *Trichomonas vaginalis*. *Infect Immun* **77**, 2703–2711.

Lamont, R. J. & Jenkinson, H. F. (1998). Life below the gum line: pathogenic mechanisms of *Porphyromonas gingivalis*. *Microbiol Mol Biol Rev* **62**, 1244–1263.

Lin, X., Wu, J. & Xie, H. (2006). *Porphyromonas gingivalis* minor fimbriae are required for cell–cell interactions. *Infect Immun* **74**, 6011–6015.

Linton, D., Allan, E., Karlyshev, A. V., Cronshaw, A. D. & Wren, B. W. (2002). Identification of *N*-acetylgalactosamine-containing glycoproteins PEB3 and CgpA in *Campylobacter jejuni*. *Mol Microbiol* **43**, 497–508.

Maeda, K., Nagata, H., Kuboniwa, M., Kataoka, K., Nishida, N., Tanaka, M. & Shizukuishi, S. (2004). Characterization of binding of *Streptococcus oralis* glyceraldehyde-3-phosphate dehydrogenase to *Porphyromonas gingivalis* major fimbriae. *Infect Immun* **72**, 5475–5477.

Mainardi, J. L., Villet, R., Bugg, T. D., Mayer, C. & Arthur, M. (2008). Evolution of peptidoglycan biosynthesis under the selective pressure of antibiotics in Gram-positive bacteria. *FEMS Microbiol Rev* **32**, 386–408.

Marraffini, L. A., Dedent, A. C. & Schneewind, O. (2006). Sortases and the art of anchoring proteins to the envelopes of Gram-positive bacteria. *Microbiol Mol Biol Rev* **70**, 192–221.

Matatov, R., Goldhar, J., Skutelsky, E., Sechter, I., Perry, R., Podschun, R., Sahly, H., Thankavel, K., Abraham, S. N. & other authors (1999). Inability of encapsulated *Klebsiella pneumoniae* to assemble functional type 1 fimbriae on their surface. *FEMS Microbiol Lett* **179**, 123–130.

McAlister, A. D., Sroka, A., Fitzpatrick, R. E., Quinsey, N. S., Travis, J., Potempa, J. & Pike, R. N. (2009). Gingipain enzymes from

Porphyromonas gingivalis preferentially bind immobilized extracellular proteins: a mechanism favouring colonization? *J Periodontal Res* **44**, 348–353.

McGraw, W. T., Potempa, J., Farley, D. & Travis, J. (1999). Purification, characterization, and sequence analysis of a potential virulence factor from *Porphyromonas gingivalis*, peptidylarginine deiminase. *Infect Immun* **67**, 3248–3256.

Mikolajczyk-Pawlinska, J., Kordula, T., Pavloff, N., Pemberton, P. A., Chen, W. C., Travis, J. & Potempa, J. (1998). Genetic variation of *Porphyromonas gingivalis* genes encoding gingipains, cysteine proteinases with arginine or lysine specificity. *Biol Chem* **379**, 205–211.

Murakami, Y., Masuda, T., Imai, M., Iwami, J., Nakamura, H., Noguchi, T. & Yoshimura, F. (2004). Analysis of major virulence factors in *Porphyromonas gingivalis* under various culture temperatures using specific antibodies. *Microbiol Immunol* **48**, 561–569.

Nagata, H., Iwasaki, M., Maeda, K., Kuboniwa, M., Hashino, E., Toe, M., Minamino, N., Kuwahara, H. & Shizukuishi, S. (2009). Identification of the binding domain of *Streptococcus oralis* glyceraldehyde-3-phosphate dehydrogenase for *Porphyromonas gingivalis* major fimbriae. *Infect Immun* **77**, 5130–5138.

Nakano, K., Nemoto, H., Nomura, R., Inaba, H., Yoshioka, H., Taniguchi, K., Amano, A. & Ooshima, T. (2009). Detection of oral bacteria in cardiovascular specimens. *Oral Microbiol Immunol* **24**, 64–68.

Nakayama, K., Yoshimura, F., Kadowaki, T. & Yamamoto, K. (1996). Involvement of arginine-specific cysteine proteinase (Arg–gingipain) in fimbriation of *Porphyromonas gingivalis*. *J Bacteriol* **178**, 2818–2824.

Nguyen, K. A., Zylicz, J., Szczesny, P., Sroka, A., Hunter, N. & Potempa, J. (2009). Verification of a topology model of PorT as an integral outer-membrane protein in *Porphyromonas gingivalis*. *Microbiology* **155**, 328–337.

Nielsen, H., Engelbrecht, J., Brunak, S. & von Heijne, G. (1997). Identification of prokaryotic and eukaryotic signal peptides and prediction of their cleavage sites. *Protein Eng* **10**, 1–6.

Nimchuk, Z., Marois, E., Kjemtrup, S., Leister, R. T., Katagiri, F. & Dangl, J. L. (2000). Eukaryotic fatty acylation drives plasma membrane targeting and enhances function of several type III effector proteins from *Pseudomonas syringae*. *Cell* **101**, 353–363.

Nishiyama, S., Murakami, Y., Nagata, H., Shizukuishi, S., Kawagishi, I. & Yoshimura, F. (2007). Involvement of minor components associated with the FimA fimbriae of *Porphyromonas gingivalis* in adhesive functions. *Microbiology* **153**, 1916–1925.

Olango, G. J., Roy, F., Sheets, S. M., Young, M. K. & Fletcher, H. M. (2003). Gingipain RgpB is excreted as a proenzyme in the *vimA*-defective mutant *Porphyromonas gingivalis* FLL92. *Infect Immun* **71**, 3740–3747.

Olsen, H. B. & Kaarsholm, N. C. (2000). Structural effects of protein lipidation as revealed by LysB29-myristoyl, des(B30) insulin. *Biochemistry* **39**, 11893–11900.

Pancholi, V. & Fischetti, V. A. (1992). A major surface protein on group A streptococci is a glyceraldehyde-3-phosphate-dehydrogenase with multiple binding activity. *J Exp Med* **176**, 415–426.

Paramonov, N., Rangarajan, M., Hashim, A., Gallagher, A., Aduse-Opoku, J., Slaney, J. M., Hounsell, E. & Curtis, M. A. (2005). Structural analysis of a novel anionic polysaccharide from *Porphyromonas gingivalis* strain W50 related to Arg-gingipain glycans. *Mol Microbiol* **58**, 847–863.

Pavloff, N., Potempa, J., Pike, R. N., Prochazka, V., Kiefer, M. C., Travis, J. & Barr, P. J. (1995). Molecular cloning and structural characterization of the Arg–gingipain proteinase of *Porphyromonas gingivalis*. Biosynthesis as a proteinase–adhesin polyprotein. *J Biol Chem* **270**, 1007–1010.

Pavloff, N., Pemberton, P. A., Potempa, J., Chen, W. C., Pike, R. N., Prochazka, V., Kiefer, M. C., Travis, J. & Barr, P. J. (1997). Molecular cloning and characterization of *Porphyromonas gingivalis* lysine-specific gingipain. A new member of an emerging family of pathogenic bacterial cysteine proteinases. *J Biol Chem* **272**, 1595–1600.

Pearson, W. R. & Lipman, D. J. (1988). Improved tools for biological sequence comparison. *Proc Natl Acad Sci U S A* **85**, 2444–2448.

Pike, R. N., Potempa, J., McGraw, W., Coetzer, T. H. & Travis, J. (1996). Characterization of the binding activities of proteinase–adhesin complexes from *Porphyromonas gingivalis*. *J Bacteriol* **178**, 2876–2882.

Potempa, J., Pike, R. & Travis, J. (1995). The multiple forms of trypsin-like activity present in various strains of *Porphyromonas gingivalis* are due to the presence of either Arg–gingipain or Lys–gingipain. *Infect Immun* **63**, 1176–1182.

Pratto, F., Suzuki, Y., Takeyasu, K. & Alonso, J. C. (2009). Single-molecule analysis of protein–DNA complexes formed during partition of newly replicated plasmid molecules in *Streptococcus pyogenes*. *J Biol Chem* **284**, 30298–30306.

Rangarajan, M., Aduse-Opoku, J., Paramonov, N., Hashim, A., Bostanci, N., Fraser, O. P., Tarelli, E. & Curtis, M. A. (2008). Identification of a second lipopolysaccharide in *Porphyromonas gingivalis* W50. *J Bacteriol* **190**, 2920–2932.

Rodriguez, S. B., Stitt, B. L. & Ash, D. E. (2009). Expression of peptidylarginine deiminase from *Porphyromonas gingivalis* in *Escherichia coli*: enzyme purification and characterization. *Arch Biochem Biophys* **488**, 14–22.

Sahly, H., Podschun, R., Oelschlaeger, T. A., Greiwe, M., Parolis, H., Hasty, D., Kekow, J., Ullmann, U., Ofek, I. & other authors (2000). Capsule impedes adhesion to and invasion of epithelial cells by *Klebsiella pneumoniae*. *Infect Immun* **68**, 6744–6749.

Salinero, K. K., Keller, K., Feil, W. S., Feil, H., Trong, S., Di, B. G. & Lapidus, A. (2009). Metabolic analysis of the soil microbe *Dechloromonas aromatica* str. RCB: indications of a surprisingly complex life-style and cryptic anaerobic pathways for aromatic degradation. *BMC Genomics* **10**, 351.

Sato, K., Sakai, E., Veith, P. D., Shoji, M., Kikuchi, Y., Yukitake, H., Ohara, N., Naito, M., Okamoto, K. & other authors (2005). Identification of a new membrane-associated protein that influences transport/maturation of gingipains and adhesins of *Porphyromonas gingivalis*. *J Biol Chem* **280**, 8668–8677.

Shirai, H., Blundell, T. L. & Mizuguchi, K. (2001). A novel superfamily of enzymes that catalyze the modification of guanidino groups. *Trends Biochem Sci* **26**, 465–468.

Shoji, M., Ratnayake, D. B., Shi, Y., Kadowaki, T., Yamamoto, K., Yoshimura, F., Akamine, A., Curtis, M. A. & Nakayama, K. (2002). Construction and characterization of a nonpigmented mutant of *Porphyromonas gingivalis*: cell surface polysaccharide as an anchorage for gingipains. *Microbiology* **148**, 1183–1191.

Shoji, M., Naito, M., Yukitake, H., Sato, K., Sakai, E., Ohara, N. & Nakayama, K. (2004). The major structural components of two cell surface filaments of *Porphyromonas gingivalis* are matured through lipoprotein precursors. *Mol Microbiol* **52**, 1513–1525.

Slakeski, N., Margetts, M., Moore, C., Czajkowski, L., Barr, I. G. & Reynolds, E. C. (2002). Characterization and expression of a novel *Porphyromonas gingivalis* outer membrane protein, Omp28. *Oral Microbiol Immunol* **17**, 150–156.

Stapleton, P. D. & Taylor, P. W. (2002). Methicillin resistance in *Staphylococcus aureus*: mechanisms and modulation. *Sci Prog* **85**, 57–72.

Stathopoulou, P. G., Galicia, J. C., Benakanakere, M. R., Garcia, C. A., Potempa, J. & Kinane, D. F. (2009). *Porphyromonas gingivalis* induce apoptosis in human gingival epithelial cells through a gingipain-dependent mechanism. *BMC Microbiol* **9**, 107.

Suzuki, Y., Yoshimura, F., Takahashi, K., Tani, H. & Suzuki, T. (1988). Detection of fimbriae and fimbrial antigens on the oral anaerobe *Bacteroides gingivalis* by negative staining and serological methods. *J Gen Microbiol* **134**, 2713–2720.

Ton-That, H., Marraffini, L. A. & Schneewind, O. (2004). Protein sorting to the cell wall envelope of Gram-positive bacteria. *Biochim Biophys Acta* **1694**, 269–278.

Tsukiji, S. & Nagamune, T. (2009). Sortase-mediated ligation: a gift from Gram-positive bacteria to protein engineering. *ChemBioChem* **10**, 787–798.

Vanterpool, E., Roy, F. & Fletcher, H. M. (2004). The *vimE* gene downstream of *vimA* is independently expressed and is involved in modulating proteolytic activity in *Porphyromonas gingivalis* W83. *Infect Immun* **72**, 5555–5564.

Vanterpool, E., Roy, F. & Fletcher, H. M. (2005a). Inactivation of *vimF*, a putative glycosyltransferase gene downstream of *vimE*, alters glycosylation and activation of the gingipains in *Porphyromonas gingivalis* W83. *Infect Immun* **73**, 3971–3982.

Vanterpool, E., Roy, F., Sandberg, L. & Fletcher, H. M. (2005b). Altered gingipain maturation in *vimA*- and *vimE*-defective isogenic mutants of *Porphyromonas gingivalis*. *Infect Immun* **73**, 1357–1366.

Vanterpool, E., Roy, F., Zhan, W., Sheets, S. M., Sangberg, L. & Fletcher, H. M. (2006). VimA is part of the maturation pathway for the major gingipains of *Porphyromonas gingivalis* W83. *Microbiology* **152**, 3383–3389.

Veith, P. D., Chen, Y. Y. & Reynolds, E. C. (2004). *Porphyromonas gingivalis* RgpA and Kgp proteinases and adhesins are C terminally processed by the carboxypeptidase CPG70. *Infect Immun* **72**, 3655–3657.

Voytas, D. & Ke, N. (2001). Detection and quantitation of radiolabeled proteins and DNA in gels and blots. *Curr Protoc Mol Biol* **Appendix 3**, Appendix 3A.

Wang, M., Liang, S., Hosur, K. B., Domon, H., Yoshimura, F., Amano, A. & Hajishengallis, G. (2009). Differential virulence and innate immune interactions of type I and II fimbrial genotypes of *Porphyromonas gingivalis*. *Oral Microbiol Immunol* **24**, 478–484.

Wright, T. L., Ellen, R. P., Lacroix, J. M., Sinnadurai, S. & Mittelman, M. W. (1997). Effects of metronidazole on *Porphyromonas gingivalis* biofilms. *J Periodontal Res* **32**, 473–477.

Yoshimura, F., Murakami, Y., Nishikawa, K., Hasegawa, Y. & Kawaminami, S. (2009). Surface components of *Porphyromonas gingivalis*. *J Periodontal Res* **44**, 1–12.

Zaas, D. W., Duncan, M., Rae, W. J. & Abraham, S. N. (2005). The role of lipid rafts in the pathogenesis of bacterial infections. *Biochim Biophys Acta* **1746**, 305–313.

Zhang, Y. (2008). I-TASSER server for protein 3D structure prediction. *BMC Bioinformatics* **9**, 40.

Zhang, Y. (2009). I-TASSER: Fully automated protein structure prediction in CASP8. *Proteins* **77** (Suppl. 9), 100–113.

Edited by: R. J. Lamont